

# Visual-Inertial SLAM for Agricultural Robotics: Benchmarking the Benefits and Computational Costs of Loop Closing

Fabian Schmidt<sup>1,2</sup> | Constantin Blessing<sup>1</sup> | MarkusENZweiler<sup>1</sup> | Abhinav Valada<sup>2</sup>

<sup>1</sup>Institute for Intelligent Systems, Esslingen  
University of Applied Sciences, Esslingen,  
Germany

<sup>2</sup>Department of Computer Science, University  
of Freiburg, Freiburg, Germany

## Correspondence

Corresponding author Fabian Schmidt.  
Email: fabian.schmidt@hs-esslingen.de

## Abstract

Simultaneous Localization and Mapping (SLAM) is essential for mobile robotics, enabling autonomous navigation in dynamic, unstructured outdoor environments without relying on external positioning systems. In agricultural applications, where environmental conditions can be particularly challenging due to variable lighting or weather conditions, Visual-Inertial SLAM has emerged as a potential solution. This paper benchmarks several open-source Visual-Inertial SLAM systems, including ORB-SLAM3, VINS-Fusion, OpenVINS, Kimera, and SVO Pro, to evaluate their performance in agricultural settings. We focus on the impact of loop closing on localization accuracy and computational demands, providing a comprehensive analysis of these systems' effectiveness in real-world environments and especially their application to embedded systems in agricultural robotics. Our contributions further include an assessment of varying frame rates on localization accuracy and computational load. The findings highlight the importance of loop closing in improving localization accuracy while managing computational resources efficiently, offering valuable insights for optimizing Visual-Inertial SLAM systems for practical outdoor applications in mobile robotics.

## KEYWORDS

Visual-Inertial SLAM, loop closing, unstructured environments, agricultural robotics

## 1 | INTRODUCTION

Simultaneous Localization and Mapping (SLAM) is a critical technology in the field of mobile robotics. SLAM enables robots to build a map of an unknown environment while simultaneously keeping track of their current location within that map. The primary purpose of SLAM is to provide autonomous robots with the ability to navigate and operate effectively in dynamic (Bešić & Valada, 2022) and unstructured environments (Capua et al., 2018; Cremona et al., 2022; Pire et al., 2019) without relying on external positioning systems. Many SLAM systems employed in agricultural applications depend on Global Navigation Satellite System (GNSS), with RTK-GNSS (Real-Time Kinematic Global Navigation Satellite System) being particularly costly and requiring extensive base station coverage to ensure accuracy (Aguiar et al., 2020). Alternative solutions leverage consumer-grade GNSS, integrating its output with various onboard sensors to improve localization accuracy (Cao et al., 2022; Cattaneo & Valada, 2024; Nayak et al., 2023; Arce et al., 2023). However, GNSS signals are not consistently available and may be unreliable due to environmental conditions, such as dense tree canopies in orchards, which can hinder signal reception and lead to catastrophic failures. Consequently, Visual-Inertial SLAM systems have

facilitated numerous applications in robotics, particularly in outdoor scenarios where GNSS reliability is compromised (Cadena et al., 2016; Gosala et al., 2023).

Outdoor scenarios, unlike urban environments, face harsh environmental conditions, e.g., seasonal changes, drastic illumination changes, large open fields, and irregular terrain, making navigation more difficult. The ability of Visual-Inertial SLAM systems to autonomously construct and update maps of their surroundings while simultaneously determining their own position has profoundly influenced the field of autonomous navigation in outdoor scenarios. However, when estimating the robot's motion over time, Visual-Inertial SLAM leads to drift, challenging practical applications. For long-duration operations, a consistent and robust system is required that demonstrates adequate resistance to drift (Angeli et al., 2008; Vödisch et al., 2022, 2023).

In Visual-Inertial SLAM systems, loop closing (LC) is a key technique to minimize drift by identifying previously visited locations. This technique corrects the robot's historical trajectory and optimizes the map estimation, enhancing both localization accuracy and map integrity over time. In agricultural tasks, where robots often operate over large and repetitive areas, LC maintains precise navigation and mapping, crucial for activities such as planting, monitoring, and harvesting (Islam et al., 2023). By identifying loops, the system can adjust the map

and the robot's position to mitigate cumulative errors. While theoretically promising, LC introduces practical challenges. It requires the system to continuously compare current observations with past data to detect overlaps, demanding substantial computational power. This demand is particularly challenging for mobile robots, where computational resources are limited, and real-time processing capability is crucial. Efficiently managing these demands is essential to maintain accurate localization without compromising performance or battery life (Zhao et al., 2020). Robust algorithms that minimize computational overhead are critical for practical applications of Visual-Inertial SLAM in mobile robotics (Tsintotas et al., 2022).

In previous research (Schmidt et al., 2024), we benchmarked several open-source Visual-Inertial SLAM systems in agricultural settings, evaluated the impact of LC on localization accuracy, and analyzed the computational demands. In this study, we expand on our results, conducting experiments to assess how varying frame rates influence localization accuracy and computational load. We evaluate two new methods, i.e., Kimera and SVO Pro, offering insights into optimizing Visual-Inertial SLAM for practical applications. Our contributions include:

1. **Benchmarking Open-Source Visual-Inertial SLAM Methods:** We conduct a comprehensive evaluation of the application of various open-source Visual-Inertial SLAM methods in unstructured outdoor environments, focusing on their performance and applicability in agricultural settings.
2. **Quantitative and Qualitative Analysis of LC Effects:** We evaluate the impact of LC on localization accuracy across diverse driving scenarios and environmental conditions, providing a detailed analysis of its benefits and limitations.
3. **Resource Analysis:** We investigate the additional computational overhead imposed by LC, highlighting the trade-offs in computational resources.
4. **Frame Rate Impact Study:** We research the impact of different frame rates on localization accuracy and computational effort, offering insights into optimizing Visual-Inertial SLAM systems for real-time applications.

The remainder of this paper is structured as follows: Section 2 reviews existing Visual and Visual-Inertial SLAM benchmarks across various environments and settings. Section 3 describes the experimental setup, detailing the specific Visual-Inertial SLAM methods used, the dataset, and the evaluation criteria. Section 4 presents the results and discusses their implications and relevance for autonomous navigation. Finally, Section 5 concludes the paper by summarizing key findings and proposing future research directions.

## 2 | RELATED WORK

The extensive literature on SLAM systems provides insights into applications, difficulties, and performance in a variety of scenarios, highlighting their significance in the development of robotic navigation. This chapter

focuses on benchmarks for Visual and Visual-Inertial SLAM, essential for the evaluation and comparison of individual SLAM performances.

Numerous benchmarks (Buyval et al., 2017; Ibragimov & Afanasyev, 2017; Filipenko & Afanasyev, 2018; Delmerico & Scaramuzza, 2018; Giubilato et al., 2018, 2019; Mingachev et al., 2020; Gao et al., 2020; Servières et al., 2021; Merzlyakov & Macenski, 2021; Bahnam et al., 2021; Bujanca et al., 2021; Herrera-Granda et al., 2023; Sharafutdinov et al., 2023; Passalis et al., 2022) systematically evaluate the localization accuracy of contemporary Visual and Visual-Inertial SLAM algorithms through the use of renowned datasets such as TUM RGB-D (Sturm et al., 2012), EuRoC (Burri et al., 2016), and KITTI (Geiger et al., 2012). These benchmarks offer insights into the efficacy of SLAM algorithms across diverse environments, from indoor spaces to unpredictable outdoor settings, incorporating various robotic platforms, such as drones, mobile robots, and cars. Furthermore, several benchmarks, such as (Delmerico & Scaramuzza, 2018), (Bahnam et al., 2021), (Giubilato et al., 2018), (Giubilato et al., 2019), (Bujanca et al., 2021), and (Sharafutdinov et al., 2023), evaluate the computational performance of SLAM algorithms in addition to localization accuracy. (Delmerico & Scaramuzza, 2018) specifically monitor CPU and RAM usage across different embedded computing platforms. (Giubilato et al., 2018, 2019) evaluated stereo Visual SLAM systems on an embedded platform, both with and without GPU support, whereas (Bahnam et al., 2021) provide detailed statistics on computational timings. In contrast, (Bujanca et al., 2021) focus on ensuring consistent localization accuracy results across various platforms, including an embedded platform, a consumer-grade laptop, and a high-end workstation. (Sharafutdinov et al., 2023) conducted an extensive evaluation of 13 Visual and Visual-Inertial SLAM algorithms, focusing on their performance and reliability in autonomous navigation for both indoor and urban outdoor scenarios, while also monitoring memory usage and CPU utilization.

In addition to common benchmarks, studies such as (Chahine & Pradalier, 2018; Joshi et al., 2019; Tschopp et al., 2019; Li et al., 2023) specifically explore Visual and Visual-Inertial SLAM applications in particular contexts, demonstrating their adaptability and potential constraints in challenging environments. (Chahine & Pradalier, 2018) utilize the Symphony Lake dataset (Griffith et al., 2017), which consists of images of a lake shore captured over three years across different seasons. They evaluated three different SLAM methods to assess the seasonal influence on localization accuracy. (Joshi et al., 2019) evaluate ten open-source Visual-Inertial SLAM algorithms in marine settings, addressing challenges such as low visibility and dynamic lighting conditions. This comprehensive analysis, using datasets from underwater robots, provides insights into the performance of direct and feature-based SLAM methods. (Tschopp et al., 2019) explore Visual Odometry methods for rail vehicles, emphasizing the combination of stereo vision with inertial measurement units (IMU) to improve the precision of motion estimation. They highlight the importance of robust algorithms that address challenges such as high velocities and constrained motion and compare various Visual-Inertial Odometry frameworks to showcase their strengths and limitations. (Li et al., 2023) explore the application

feasibility of monocular Visual-Inertial SLAM methods in freight railways. They emphasize challenges including scale estimation errors and frequent failures attributed to the constrained motion patterns.

Benchmarks in agricultural environments highlight the specific challenges of implementing SLAM technologies, which must adapt to dynamic conditions and complex landscapes. (Capua et al., 2018) study the application of Visual SLAM in orange orchards, highlighting the need for systems capable of adapting to the diverse and cluttered environments typical for agriculture. (Hroob et al., 2021) evaluate Visual SLAM systems in a simulated vineyard, demonstrating SLAM’s potential in precision agriculture. Their study focuses on the challenges posed by the vineyard’s structured yet dynamic environment, including varying vine heights and the influence of changing sunlight throughout the day. (Comelli et al., 2019) and the follow-up (Cremona et al., 2022) cover state-of-the-art stereo Visual-Inertial SLAM systems on an arable farming dataset (Pire et al., 2019), specifically in soybean fields. These studies highlight the operational challenges faced by using SLAM in agricultural contexts, evaluating their accuracy and robustness. They also address the adaptability of SLAM systems to the distinct characteristics of arable farming, such as crop height variability and environmental factors such as wind and lighting conditions.

In this paper, we aim to address key gaps in the existing literature by focusing on unstructured outdoor environments such as gardens or parks, which have been underrepresented in current benchmarks. These environments present distinct challenges for SLAM technologies, including highly variable vegetation density, uneven terrain, and fluctuating lighting conditions due to canopy coverage. Unlike traditional agricultural settings that have been explored in existing benchmarks (Capua et al., 2018; Hroob et al., 2021; Comelli et al., 2019; Cremona et al., 2022), which often deal with structured row crops and controlled variables, gardens and parks offer a more dynamic and unpredictable landscape. This necessitates the development of more adaptable and robust SLAM algorithms capable of handling sudden environmental changes and less predictable pathways. Furthermore, our approach includes a detailed study of the interplay between environmental complexity and SLAM system performance, providing insights into how these factors influence the operational efficacy of robotic navigation. By exploring these unique settings, our research contributes to a broader understanding of SLAM applicability and enhances the technology’s adaptability to diverse agricultural and natural environments.

### 3 | EXPERIMENTAL SETUP

In this section, we first describe the dataset that we use for benchmarking. Second, we introduce the selected Visual-Inertial SLAM algorithms chosen for evaluation on the aforementioned dataset. Finally, we describe the evaluation methodology in more detail.

#### 3.1 | Dataset

For data recording, we utilized an unmanned ground vehicle (UGV) designed for remote control, which provides the necessary mobility and versatility required to navigate the environments effectively. The UGV was equipped with an Intel RealSense T265 camera, augmented with a six degrees of freedom (DOF) IMU. The camera captures imagery at a frequency of 30 Hz with a resolution of 848x800 pixels, employing a monochrome global shutter and a fisheye lens with a 160° diagonal field of view. The IMU records data with the accelerometer at 62.5 Hz and the gyroscope at 200 Hz. The accuracy and reliability of data in visual localization studies are critically dependent on the quality of the ground truth data. To ensure high-precision ground truth for the robot’s positioning, a Leica TS-16 Total Station was employed. It captures the robot’s position using a prism mounted firmly on the robot’s sensor board. The total station records three DOF positional ground truth data at a frequency of 2-5 Hz, which is sufficient given the UGV’s speed of approximately 1 km/h. This setup ensures positional accuracy at the millimeter level. The recorded trajectory consists of a series of data points, each comprising a timestamp and the three-dimensional position of the robot.

We recorded 8 sequences, focusing on 4 unstructured outdoor environments that encompass diverse garden sizes and a park-like expanse, as depicted in Figure 1. Additionally, we considered different driving scenarios that can be divided into two categories: *Perimeter* and *Lane*. In the *Perimeter* scenario, the robot completes three full rounds starting from the edge of the lawn area, ensuring that the boundaries of the area are clearly defined and consistently maintained throughout the operation. Conversely, in the *Lane* scenario, the robot moves in parallel lanes across the lawn, incorporating multiple 180° turns, resembling a methodical, straight-line path. This approach is efficient for large, regular-shaped lawns, providing uniform coverage and efficient use of time and resources.

By covering these scenarios, we aim to provide the data to identify the effect of driving strategy on localization accuracy. Importantly, each scenario introduces a different number of rotations and movements that can potentially affect the precision of the robot’s localization system. Understanding the impact of these variables is crucial for optimizing the robot’s navigation and operational efficiency. Further information on the different locations and driving scenarios is shown in Table 1.

#### 3.2 | Algorithms

For this benchmark, we exclusively focus on open-source Visual-Inertial SLAM algorithms that utilize stereo cameras and the ROS (Robot Operating System) framework, containing an LC module. As shown in Table 2, we selected methods that are most diverse regarding their techniques in frontend, backend, and LC to gain a comprehensive understanding of their influence on performance.



**FIGURE 1** Different dataset recording environments. Top left shows the *Garden Small*, top right *Garden Medium*, bottom left *Garden Large* and bottom right *Park* location.

**TABLE 1** Dataset characteristics.

| Location      | Scenario  | Duration [s] | Distance [m] |
|---------------|-----------|--------------|--------------|
| Garden Small  | Lane      | 189.0        | 45.2         |
|               | Perimeter | 361.1        | 125.6        |
| Garden Medium | Lane      | 264.3        | 89.0         |
|               | Perimeter | 466.6        | 167.4        |
| Garden Large  | Lane      | 352.8        | 123.4        |
|               | Perimeter | 788.1        | 299.2        |
| Park          | Lane      | 210.2        | 43.4         |
|               | Perimeter | 437.9        | 164.2        |

**TABLE 2** Overview of the Visual-Inertial SLAM methods and their respective components.

| Method                                | Frontend    | Backend      | LC             |
|---------------------------------------|-------------|--------------|----------------|
| ORB-SLAM3                             | Feature     | Optimization | PGO + BA       |
| VINS-Fusion                           | Feature     | Optimization | PGO            |
| OpenVINS<br>+ VINS-Fusion<br>+ Maplab | Feature     | Filter       | -<br>PGO<br>BA |
| Kimera                                | Feature     | Optimization | PGO            |
| SVO Pro                               | Semi-Direct | Optimization | PGO, BA        |

**ORB-SLAM3** (Campos et al., 2021) stands out as a multimodal feature- and optimization-based approach with an integrated LC mechanism. The system operates through three threads: tracking, local mapping, and loop and map merging. In the front end, ORB-SLAM3 uses a feature-based approach by extracting ORB features (Rublee et al.,

2011). The tracking thread determines the current frame's pose by minimizing reprojection errors with ORB features and selects keyframes. Optimization-based methods are employed in the backend. The local mapping thread enhances the map by adjusting keyframes locally using local bundle adjustment (BA). Finally, the loop and map merging thread identifies revisited areas using a bag-of-words (Gálvez-López & Tardós, 2012) keyframe database and performs loop closures to ensure map accuracy by applying pose graph optimization (PGO) followed by global bundle adjustment.

**VINS-Fusion** (Qin et al., 2019) offers a versatile sensor fusion framework that leverages both visual and inertial cues for state estimation. Employing a feature-based approach in the frontend, VINS-Fusion extracts and matches visual features from camera images. The backend integrates an optimization-based state estimation module, which calculates the device's pose by fusing data from cameras and IMUs, ensuring accurate trajectory and orientation determination. The mapping module further refines this information by integrating environmental features and enhancing spatial awareness. VINS-Fusion includes an LC module that identifies previously visited locations and uses global optimization, specifically PGO, to minimize drift over time.

**OpenVINS** (Geneva et al., 2020) is a filter-based method for visual-inertial navigation, utilizing tightly-coupled integration of camera and IMU data for precise state estimation. In the front end, it tracks visual features from camera images using a feature-based approach. The backend incorporates a Multi-State Constrained Kalman Filter (MSCKF) (Mourikis & Roumeliotis, 2007) and sliding window optimization to efficiently handle high-frequency IMU data and visual inputs for accurate updates to poses and velocities. While OpenVINS does not include LC

by default, its modular design allows for the integration of the LC module from VINS-Fusion. Furthermore, Maplab (Cramariuc et al., 2022) can enhance OpenVINS by adding offline Loop Closing capabilities. The maps and states estimated by OpenVINS are post-processed and further refined using Maplab’s optimization and loop closure detection tools, facilitating global BA.

**Kimera** (Rosinol et al., 2021) provides a comprehensive framework that combines Visual-Inertial Odometry with metric-semantic mapping for enhanced scene understanding. Kimera uses a feature-based approach in the front end, extracting and matching visual features from camera images. The backend relies on optimization-based methods to refine pose estimates and construct a semantically rich map of the environment. The Visual-Inertial Odometry module estimates the device’s trajectory by tightly integrating visual and inertial data, while the metric-semantic mapping module improves spatial awareness by incorporating geometric and semantic information. Kimera also features an LC module that identifies previously visited locations and applies PGO.

**SVP Pro** (Forster et al., 2017) is a flexible framework for visual-inertial navigation, capable of operating in both monocular and stereo-inertial configurations. The system uses a semi-direct approach in the front end, minimizing photometric error from image intensities and incorporating feature extraction for robust pose estimation. A probabilistic depth estimation algorithm ensures efficient tracking of pixels on weak corners and edges. In the backend, the estimated poses are optimized for accuracy and consistency. SVP Pro supports both PGO and BA, but since BA is not robustly implemented for stereo-inertial configurations, only PGO is used in this work.

Since our testing conditions differ from the default examples provided by these methods, careful parameter tuning was essential. To ensure robust performance in our unique environment, we empirically tuned the frontend parameters of each SLAM algorithm.

### 3.3 | Evaluation Metrics and Criteria

In Visual and Visual-Inertial SLAM systems, maintaining the global accuracy of the predicted trajectory is crucial. This accuracy is evaluated by measuring the absolute and relative differences between the estimated trajectory and the ground truth trajectory. Since these trajectories may be presented in different coordinate systems, they must be aligned first. Umeyama’s method (Umeyama, 1991) can be used to solve this alignment in closed form. The method identifies the transformation that yields the optimal least-squares solution to map the estimated trajectory onto the ground truth trajectory.

We compute the root mean squared (RMSE) absolute trajectory error (ATE) as one of the main metrics to quantify the deviation between estimated and ground truth positions. The ATE measures the global consistency of the estimated trajectory, reflecting the overall difference between the estimated and ground truth positions after alignment. In addition to ATE, we compute the RMSE relative pose error (RPE) to evaluate the local accuracy of the SLAM algorithms over short intervals. The RPE measures the error in the relative transformations between

consecutive poses, thus, evaluating the local accuracy and consistency of the trajectory. For the calculation of both ATE and RPE, we follow the methodologies described in (Sturm et al., 2012). We further analyze CPU and memory utilization to understand the computational demands of each Visual-Inertial SLAM method and LC. Since we rely on ROS-based algorithms, the CPU and memory utilization of the corresponding ROS nodes can be determined accurately.

To verify the reliability and reproducibility of our results, we evaluate the SLAM algorithms by conducting five trials on each dataset sequence before calculating the average RMSE ATE and RPE using the open-source evaluation toolbox Evo (Grupp, 2017). We filter out invalid trajectories to ensure the accuracy and reliability of the analysis by excluding failed runs. The criteria for filtering invalid trajectories include:

- **Scenario Duration Coverage:** Runs with valid pose estimates in less than 80% of the scenario duration are considered failures. Thus, only trajectories with sufficient coverage and consistency are analyzed.
- **Pose Frequency:** Runs must produce at least one pose per second to be deemed successful, ensuring adequate temporal resolution for precise tracking.

Trajectories failing to meet these criteria are excluded from further analysis. This process is essential for maintaining data integrity and focusing on runs that adequately reflect the SLAM systems’ performance. We conducted all experiments on an Intel Core i9-13900HX with 64 GB RAM, operating within a Docker container based on Ubuntu 20.04 and ROS Noetic.

## 4 | EXPERIMENTAL EVALUATIONS

In this section, we present the results from the experiments. We investigate the influence of implementing LC on the localization accuracy and computational demands of various SLAM algorithms. All methods are used in stereo-inertial mode, operating on the data provided by the Intel RealSense T265.

### 4.1 | Localization Accuracy

To evaluate the localization accuracy of the SLAM algorithms, we focus on both quantitative metrics and qualitative observations.

#### 4.1.1 | Quantitative Results

We use the ATE and RPE metrics to evaluate global and local localization accuracy, respectively. Tables 3 and 4 present the RMSE ATE and RMSE RPE for the evaluated SLAM algorithms across the different scenarios.

**ORB-SLAM3** exhibited consistent performance with and without LC across different frame rates in multiple environments, particularly maintaining low ATE values for both *Perimeter* and *Lane* scenarios. In the

**TABLE 3** RMSE ATE [m] across different environments with and without LC at 30 FPS, 15 FPS, and 5 FPS for the *Perimeter* (P) and *Lane* (L) scenario. An 'x' indicates that the method failed, either due to no valid results being available or errors exceeding 100 meters, implying significant drift and unreliable position estimation in the tested environments. To calculate the scenario-specific mean average, values were only considered when results were reported across all FPS and LC configurations of the method. The best method-specific result is in bold, with the top three results across all methods highlighted as **best**, **second**, and **third**.

| Method                    | FPS | LC  | Garden Small |             | Garden Medium |             | Garden Large |              | Park        |              | Average     |             |
|---------------------------|-----|-----|--------------|-------------|---------------|-------------|--------------|--------------|-------------|--------------|-------------|-------------|
|                           |     |     | P            | L           | P             | L           | P            | L            | P           | L            | P           | L           |
| ORB-SLAM3                 | 30  | On  | <b>0.24</b>  | 0.19        | 0.64          | x           | <b>1.68</b>  | <b>0.36</b>  | <b>0.65</b> | <b>0.26</b>  | <b>0.51</b> | 0.19        |
|                           |     | Off | <b>0.24</b>  | <b>0.18</b> | 0.75          | x           | x            | <b>0.80</b>  | 0.68        | 0.30         | 0.56        | <b>0.18</b> |
|                           | 15  | On  | <b>0.25</b>  | 0.19        | <b>0.60</b>   | x           | 1.69         | <b>0.36</b>  | <b>0.67</b> | 0.33         | <b>0.51</b> | 0.19        |
|                           |     | Off | 0.28         | <b>0.18</b> | 0.73          | x           | x            | <b>1.62</b>  | 0.70        | 0.38         | 0.57        | <b>0.18</b> |
|                           | 5   | On  | <b>0.26</b>  | 0.50        | 0.85          | x           | x            | x            | 2.58        | x            | 1.23        | 0.50        |
|                           |     | Off | 0.30         | 0.61        | 1.45          | x           | 1.89         | x            | 3.27        | x            | 1.67        | 0.61        |
| VINS-Fusion               | 30  | On  | 1.64         | x           | 2.02          | <b>0.58</b> | 3.90         | x            | <b>0.79</b> | <b>20.70</b> | <b>1.41</b> | <b>0.58</b> |
|                           |     | Off | 1.69         | <b>0.21</b> | 2.08          | 0.59        | 4.00         | x            | 1.81        | 24.86        | 1.94        | 0.59        |
|                           | 15  | On  | <b>1.47</b>  | x           | <b>1.94</b>   | 1.36        | <b>3.86</b>  | <b>19.65</b> | 1.63        | 92.37        | 1.79        | 1.36        |
|                           |     | Off | 1.51         | x           | 2.00          | 1.37        | 3.89         | 19.81        | 2.74        | 89.40        | 2.37        | 1.37        |
|                           | 5   | On  | x            | x           | 2.43          | 2.64        | x            | x            | 15.89       | x            | 9.16        | 2.64        |
|                           |     | Off | x            | x           | 2.87          | 2.89        | x            | x            | 16.69       | x            | 9.78        | 2.89        |
| OpenVINS<br>+ VINS-Fusion | 30  | On  | 0.50         | x           | 0.82          | <b>0.35</b> | <b>0.75</b>  | x            | <b>1.58</b> | <b>0.19</b>  | <b>0.91</b> | <b>0.19</b> |
|                           |     | Off | 0.52         | x           | 1.02          | 0.41        | 0.95         | x            | 1.67        | 0.31         | 1.04        | 0.31        |
|                           | 15  | On  | 0.49         | x           | 0.82          | x           | <b>0.75</b>  | x            | <b>1.58</b> | <b>0.19</b>  | <b>0.91</b> | <b>0.19</b> |
|                           |     | Off | 0.51         | x           | 1.02          | x           | 0.95         | x            | 1.67        | 0.31         | 1.04        | 0.31        |
|                           | 5   | On  | <b>0.45</b>  | x           | <b>0.64</b>   | x           | 1.46         | x            | 1.80        | 0.33         | 1.09        | 0.33        |
|                           |     | Off | 0.58         | x           | 0.86          | x           | 1.81         | x            | 1.93        | 0.36         | 1.29        | 0.36        |
| OpenVINS<br>+ Maplab      | 30  | On  | 0.32         | <b>0.20</b> | <b>0.43</b>   | <b>0.22</b> | <b>0.65</b>  | 5.63         | <b>0.56</b> | <b>0.17</b>  | <b>0.49</b> | <b>0.20</b> |
|                           |     | Off | 0.61         | 0.26        | 1.24          | 0.40        | 1.06         | <b>4.93</b>  | 1.63        | <b>0.17</b>  | 1.13        | 0.28        |
|                           | 15  | On  | <b>0.27</b>  | <b>0.18</b> | 0.44          | 0.23        | <b>0.66</b>  | 8.19         | 0.76        | <b>0.19</b>  | <b>0.53</b> | <b>0.20</b> |
|                           |     | Off | 0.59         | 0.26        | 1.24          | 0.40        | 1.06         | 6.63         | 1.63        | <b>0.19</b>  | 1.13        | 0.28        |
|                           | 5   | On  | 0.71         | 0.81        | 0.91          | 0.84        | 1.56         | x            | 1.76        | 0.81         | 1.24        | 0.82        |
|                           |     | Off | 0.68         | 0.19        | 0.98          | 0.87        | 2.03         | x            | 2.17        | 0.33         | 1.47        | 0.46        |
| Kimera                    | 30  | On  | 1.69         | 7.82        | 3.50          | 91.41       | 11.67        | x            | x           | 50.14        | 5.62        | 50.14       |
|                           |     | Off | 1.02         | x           | 1.90          | x           | 6.75         | x            | 21.89       | 31.87        | 3.22        | 31.87       |
|                           | 15  | On  | 2.75         | x           | 2.76          | <b>6.81</b> | 9.58         | x            | 22.91       | 17.53        | 5.03        | 17.53       |
|                           |     | Off | <b>0.99</b>  | <b>0.47</b> | <b>1.72</b>   | 22.30       | <b>5.28</b>  | x            | <b>4.34</b> | 31.39        | <b>2.66</b> | 31.39       |
|                           | 5   | On  | 6.87         | x           | 6.24          | x           | 16.86        | x            | x           | 45.79        | 9.99        | 45.79       |
|                           |     | Off | 6.09         | 9.55        | 3.96          | x           | 29.99        | x            | 62.99       | <b>2.96</b>  | 13.35       | <b>2.96</b> |
| SVO Pro                   | 30  | On  | <b>1.15</b>  | <b>0.29</b> | <b>1.48</b>   | <b>1.14</b> | <b>3.49</b>  | x            | <b>2.14</b> | <b>0.61</b>  | <b>2.49</b> | x           |
|                           |     | Off | 1.29         | 0.31        | 1.59          | x           | 4.18         | x            | 2.32        | 0.69         | 2.88        | x           |
|                           | 15  | On  | 1.56         | 0.39        | 2.06          | x           | 4.33         | x            | 2.83        | 1.01         | 3.19        | x           |
|                           |     | Off | 1.80         | 0.96        | 2.06          | x           | 5.23         | x            | 2.71        | 1.14         | 3.64        | x           |
|                           | 5   | On  | x            | x           | 8.66          | x           | 58.82        | x            | x           | x            | 33.74       | x           |
|                           |     | Off | x            | x           | 34.37         | x           | 51.00        | x            | x           | x            | 42.68       | x           |

*Garden Small* environment, the *Perimeter* scenario presented stable results for the different configurations, with only a minor increase of ATE in lower frame rates. In contrast, the performance of the *Lane* scenario significantly declined at 5 FPS, although a very low ATE was achieved at higher frame rates. In the *Garden Medium* environment, challenges were more pronounced, especially for the *Lane* scenario, which failed consistently. The *Perimeter* scenario performed better with LC and higher

frame rates. In the *Garden Large* environment, the method faces challenges in the *Perimeter* scenario with high ATE values and partial failures. However, LC significantly improves ATE in the *Lane* scenario at higher frame rates, though it fails entirely at lower frame rates. The *Park* environment showed better performance with higher frame rates, with LC providing some improvement, although challenges persisted at lower frame rates. RPE remained low with LC across all environments but

**TABLE 4** RMSE RPE [m] per meter across different environments with and without LC at 30 FPS, 15 FPS, and 5 FPS in the *Perimeter* (P) and *Lane* (L) scenario. An 'x' indicates that the method failed, either due to no valid results being available or errors exceeding 1 meter, implying significant drift and unreliable position estimation in the tested environments. To calculate the scenario-specific mean average, values were only considered when results were reported across all FPS and LC configurations of the method.

| Method                    | FPS | LC  | Garden Small |      | Garden Medium |      | Garden Large |      | Park |      | Average |      |
|---------------------------|-----|-----|--------------|------|---------------|------|--------------|------|------|------|---------|------|
|                           |     |     | P            | L    | P             | L    | P            | L    | P    | L    | P       | L    |
| ORB-SLAM3                 | 30  | On  | 0.09         | 0.16 | 0.07          | x    | 0.10         | 0.10 | 0.09 | 0.13 | 0.09    | 0.16 |
|                           |     | Off | 0.09         | 0.17 | 0.08          | x    | 0.16         | 0.12 | 0.09 | 0.15 | 0.10    | 0.17 |
|                           | 15  | On  | 0.09         | 0.17 | 0.07          | x    | 0.12         | 0.10 | 0.10 | 0.15 | 0.10    | 0.17 |
|                           |     | Off | 0.09         | 0.16 | 0.07          | x    | 0.15         | 0.14 | 0.11 | 0.18 | 0.10    | 0.16 |
|                           | 5   | On  | 0.09         | 0.17 | 0.10          | x    | 0.25         | x    | 0.27 | x    | 0.18    | 0.17 |
|                           |     | Off | 0.09         | 0.18 | 0.12          | x    | 0.19         | 0.23 | 0.35 | x    | 0.19    | 0.18 |
| VINS-Fusion               | 30  | On  | 0.17         | x    | 0.14          | 0.11 | 0.13         | 0.33 | 0.14 | 0.32 | 0.14    | 0.22 |
|                           |     | Off | 0.18         | 0.17 | 0.13          | 0.12 | 0.13         | 0.36 | 0.14 | 0.31 | 0.15    | 0.24 |
|                           | 15  | On  | 0.13         | x    | 0.13          | 0.16 | 0.13         | 0.21 | 0.18 | 0.39 | 0.14    | 0.19 |
|                           |     | Off | 0.13         | 0.25 | 0.13          | 0.16 | 0.13         | 0.20 | 0.18 | 0.38 | 0.14    | 0.18 |
|                           | 5   | On  | 0.78         | x    | 0.23          | 0.23 | 0.53         | 0.21 | 0.36 | x    | 0.48    | 0.22 |
|                           |     | Off | 0.18         | 0.30 | 0.25          | 0.25 | 0.31         | 0.20 | 0.34 | 0.96 | 0.27    | 0.22 |
| OpenVINS<br>+ VINS-Fusion | 30  | On  | 0.13         | x    | 0.13          | 0.11 | 0.08         | 0.20 | 0.25 | 0.12 | 0.15    | 0.14 |
|                           |     | Off | 0.13         | x    | 0.12          | 0.15 | 0.13         | 0.24 | 0.24 | 0.11 | 0.15    | 0.17 |
|                           | 15  | On  | 0.12         | x    | 0.13          | 0.24 | 0.08         | 0.19 | 0.25 | 0.10 | 0.15    | 0.18 |
|                           |     | Off | 0.14         | x    | 0.12          | 0.23 | 0.13         | 0.24 | 0.24 | 0.14 | 0.16    | 0.20 |
|                           | 5   | On  | 0.13         | x    | 0.11          | 0.31 | 0.13         | 0.24 | 0.20 | 0.17 | 0.14    | 0.24 |
|                           |     | Off | 0.12         | x    | 0.11          | 0.36 | 0.13         | 0.23 | 0.23 | 0.23 | 0.15    | 0.27 |
| OpenVINS<br>+ Maplab      | 30  | On  | 0.11         | 0.13 | 0.10          | 0.10 | 0.10         | 0.19 | 0.15 | 0.14 | 0.12    | 0.12 |
|                           |     | Off | 0.13         | 0.15 | 0.13          | 0.10 | 0.09         | 0.20 | 0.23 | 0.10 | 0.15    | 0.12 |
|                           | 15  | On  | 0.11         | 0.12 | 0.11          | 0.10 | 0.11         | 0.21 | 0.16 | 0.15 | 0.12    | 0.12 |
|                           |     | Off | 0.13         | 0.15 | 0.13          | 0.10 | 0.09         | 0.23 | 0.23 | 0.10 | 0.14    | 0.12 |
|                           | 5   | On  | 0.14         | 0.26 | 0.10          | 0.17 | 0.12         | 0.32 | 0.14 | 0.62 | 0.12    | 0.35 |
|                           |     | Off | 0.13         | 0.15 | 0.13          | 0.22 | 0.14         | x    | 0.22 | 0.16 | 0.16    | 0.17 |
| Kimera                    | 30  | On  | 0.18         | x    | 0.18          | 0.25 | 0.22         | 0.33 | 0.53 | 0.81 | 0.28    | 0.46 |
|                           |     | Off | 0.16         | 0.21 | 0.16          | 0.25 | 0.20         | 0.29 | 0.41 | 0.64 | 0.23    | 0.39 |
|                           | 15  | On  | 0.21         | x    | 0.21          | 0.36 | 0.21         | 0.29 | 0.44 | 0.69 | 0.27    | 0.45 |
|                           |     | Off | 0.16         | 0.21 | 0.18          | 0.32 | 0.19         | 0.39 | 0.38 | 0.69 | 0.23    | 0.47 |
|                           | 5   | On  | 0.27         | x    | 0.28          | 0.46 | 0.34         | 0.55 | 0.88 | 0.79 | 0.44    | 0.60 |
|                           |     | Off | 0.24         | 0.32 | 0.27          | 0.41 | 0.43         | 0.66 | 0.83 | 0.61 | 0.44    | 0.50 |
| SVO Pro                   | 30  | On  | 0.14         | 0.16 | 0.14          | 0.34 | 0.16         | 0.26 | 0.17 | 0.14 | 0.15    | 0.22 |
|                           |     | Off | 0.14         | 0.16 | 0.15          | 0.20 | 0.16         | 0.28 | 0.17 | 0.14 | 0.15    | 0.19 |
|                           | 15  | On  | 0.17         | 0.17 | 0.16          | 0.73 | 0.19         | 0.26 | 0.20 | 0.19 | 0.18    | 0.34 |
|                           |     | Off | 0.17         | 0.18 | 0.15          | 0.63 | 0.20         | 0.32 | 0.20 | 0.19 | 0.18    | 0.33 |
|                           | 5   | On  | 0.40         | 0.40 | 0.39          | 0.95 | 0.41         | 0.38 | 0.38 | 0.45 | 0.39    | 0.54 |
|                           |     | Off | 0.40         | 0.36 | 0.41          | 0.95 | 0.42         | 0.37 | 0.42 | 0.49 | 0.41    | 0.54 |

increased at lower frame rates and without LC, particularly in more complex environments such as *Garden Large* and *Park*. Overall, ORB-SLAM3 benefits significantly from LC and higher frame rates across all tested environments, with LC providing a notable decrease in ATE for both *Lane* and *Perimeter* scenarios.

**VINS-Fusion** showed similar performance across multiple environments. LC consistently improved results in both *Perimeter* and *Lane* scenarios, particularly at higher frame rates. In the *Garden Small*, the *Perimeter* scenario performed better at 15 FPS compared to 30 FPS,

with LC slightly reducing the ATE. The *Lane* scenario struggled across all frame rates, with significant challenges at lower frame rates. In the *Garden Medium* environment, LC reduced ATE for both scenarios. While lower frame rates increased ATE in the *Perimeter* scenario, the performance at 30 FPS and 15 FPS remained comparable. The *Lane* scenario's ATE increased significantly as the frame rate decreased. In the *Garden Large*, LC lowered ATE for the *Perimeter* scenario, showing comparable performance at 30 FPS and 15 FPS. However, the algorithm failed for the *Lane* scenario at 30 FPS and for both scenarios at 5 FPS. In the *Park*

environment, LC improved results for the *Perimeter* scenario, but ATE increased significantly as the frame rate decreased. The *Lane* scenario consistently showed poor performance, failing at lower frame rates. RPE results indicated good local accuracy with LC, especially at higher frame rates. Lower frame rates led to higher RPE values, in particular in the *Garden Small*, *Garden Medium*, and *Park* environments. Overall, VINS-Fusion performed best at 30 FPS with LC, which reduced both ATE and RPE. However, the algorithm encountered difficulties at lower frame rates and in the *Lane* scenario across different environments.

**OpenVINS + VINS-Fusion** with LC performed consistently well in the *Garden Small* and *Garden Medium* environments for the *Perimeter* scenario, showing comparable ATE at 30 FPS and 15 FPS, and the lowest ATE at 5 FPS with LC. The *Lane* scenario failed across multiple scenarios and frame rates only succeeding at 30 FPS in the *Garden Medium* and for the *Park* scenario. In the *Garden Large*, LC helped reduce ATE for the *Perimeter* scenario, remaining consistent at 30 FPS and 15 FPS but increasing significantly at 5 FPS. In the *Park* environment, LC improved ATE results, with similar performance at 30 FPS and 15 FPS. Lowering the frame rate to 5 FPS increased ATE for both scenarios. For OpenVINS + VINS-Fusion, the RPE indicated good local accuracy in the *Perimeter* scenario across all environments and frame rates. However, the method struggled with lower frame rates resulting in increased RPE values, particularly in the *Lane* scenario, but specifically failed across all frame rates in the *Garden Small* environment. Overall, OpenVINS + VINS-Fusion performed best at higher frame rates with LC, maintaining lower ATE and RPE values, but struggled with the *Lane* scenarios and lower frame rates.

**OpenVINS + Maplab** demonstrated better performance with LC for multiple environments at higher frame rates. In the *Garden Small* environment, LC effectively reduced ATE for both *Perimeter* and *Lane* scenarios at 30 FPS and 15 FPS. In the *Garden Medium* environment, performance declined notably at 5 FPS, especially for the *Lane* scenario. In the *Garden Large* environment, LC reduced ATE for the *Perimeter* scenario at 30 FPS and 15 FPS, but the *Lane* scenario struggled, particularly at lower frame rates where it failed completely. In the *Park* environment, the *Perimeter* scenario consistently showed lower ATE with LC at higher frame rates, while the *Lane* scenario's ATE was not significantly impacted by LC and increased at 5 FPS. RPE results indicated that LC helped maintain low values at high frame rates, with higher RPE values without LC, and at lower frame rates in complex environments. Overall, OpenVINS + Maplab performed well with LC, particularly at higher frame rates, but struggled in complex scenarios and at lower frame rates.

**Kimera's** performance showed consistently high ATE values across the different environments, particularly struggling in the *Lane* scenario. In the *Garden Small* environment, ATE increased with LC and worsened at lower frame rates. In the *Garden Medium* and *Garden Large* environments, ATE increased significantly and often failed for the *Lane* scenarios. The *Park* environment saw irregular performance across frame rates with very high ATE values. RPE results also highlighted local accuracy challenges, with RPE values higher with LC across most scenarios and significantly increasing at 5 FPS. Overall, Kimera struggled with both

ATE and RPE in the *Lane* scenarios and larger environments, with LC often worsening these issues.

**SVO Pro** showed improved performance with LC in various environments, particularly at higher frame rates. For the *Garden Small* environment, LC effectively lowered ATE for both *Perimeter* and *Lane* scenarios, notably at 15 FPS. The *Garden Medium* environment had a lower ATE for the *Perimeter* scenario with LC at 30 FPS and 5 FPS, whereas the *Lane* scenario struggled significantly. In the *Garden Large* environment, LC improved ATE for the *Perimeter* scenario, with lower ATE at higher frame rates, while the *Lane* scenario failed completely. In the *Park* environment, ATE reduced with LC at 30 FPS, but performance degraded as frame rates decreased, with both scenarios failing at 5 FPS. RPE results indicated reasonable local accuracy with LC, increasing slightly without LC and significantly at lower frame rates, particularly in the *Garden Medium* and *Park*. Overall, SVO Pro benefits from LC and higher frame rates, but struggles at lower frame rates and in complex environments.

#### 4.1.2 | Qualitative Results

We qualitatively evaluate the SLAM algorithms by comparing the trajectories they generated across all environments. Specifically, we evaluate ORB-SLAM3, VINS-Fusion, OpenVINS + VINS-Fusion, OpenVINS + Maplab, SVO Pro, and Kimera at 30 FPS with LC against the ground truth, see Figures 2 to 6 (a). Additionally, we present the trajectories of a selected method under various frame rates and LC configurations, as illustrated in Figures 2 through 6 (b).

In the *Garden Small Perimeter* scenario, ORB-SLAM3, OpenVINS with Maplab, and OpenVINS with VINS-Fusion demonstrated trajectories close to the ground truth, showing good resistance to drift over time, see Figure 2a. Conversely, SVO Pro, VINS-Fusion, and Kimera experienced significant drift. When comparing different LC and FPS configurations of OpenVINS + Maplab, we observed that at 30 FPS and 15 FPS, LC helped to produce highly accurate results, while without LC, the algorithms struggled with scale, see Figure 2b. At 5 FPS, significant issues arose in both scenarios, particularly during rotations.

For the *Garden Medium Perimeter* scenario, Maplab generated very accurate trajectories, whereas ORB-SLAM3 and OpenVINS + VINS-Fusion were accurate but had minor scale issues. SVO Pro and VINS-Fusion struggled with scale and minor drift, and Kimera encountered substantial drift, as visualized in Figure 3a. Across different frame rates and LC configurations of ORB-SLAM3, we observed minor drift without LC at 30 FPS and 15 FPS. We further observed that drift increased significantly at 5 FPS, especially without LC, emphasizing the importance of LC at lower frame rates, see Figure 3b.



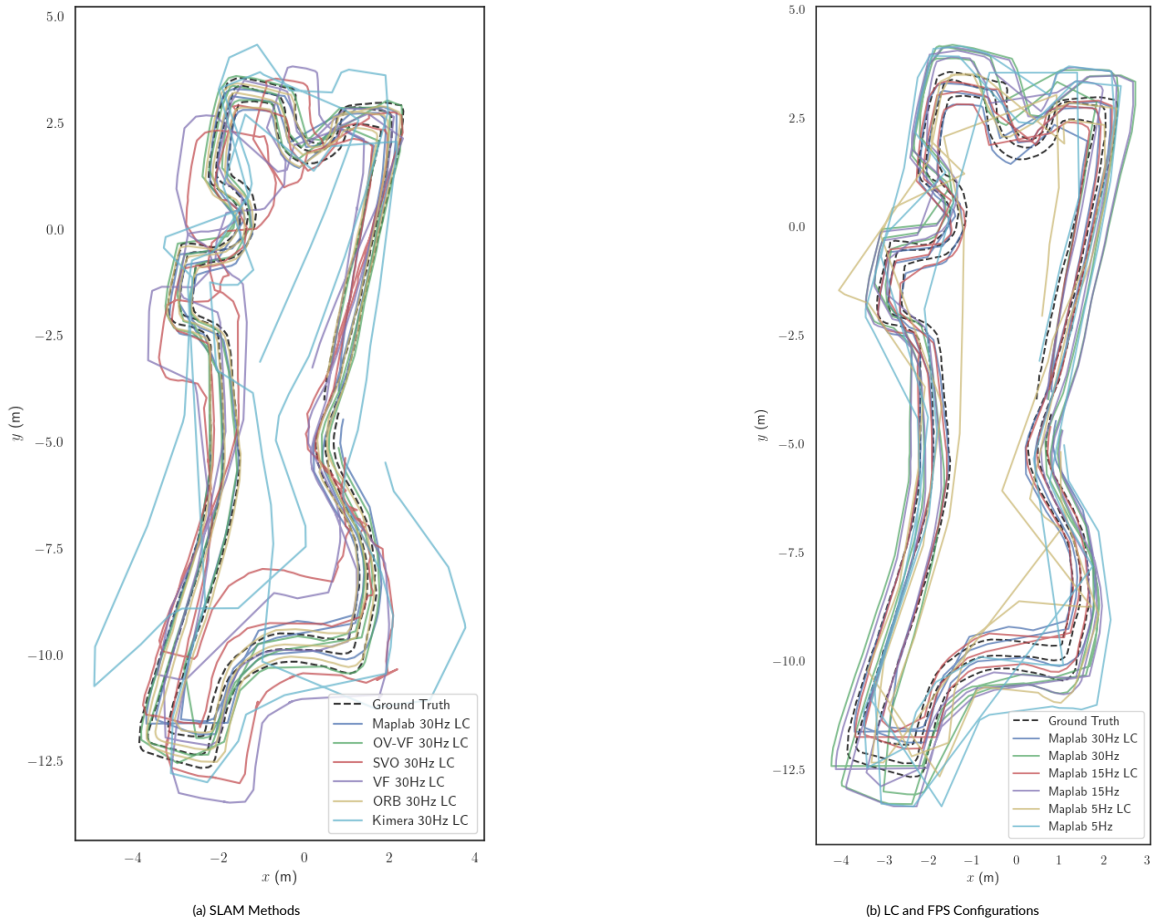


**FIGURE 2** Trajectories for the *Garden Small Perimeter* scenario: (a) illustrates the comparison of the SLAM methods while (b) shows the differences in LC and FPS configurations of OpenVINS + Maplab.

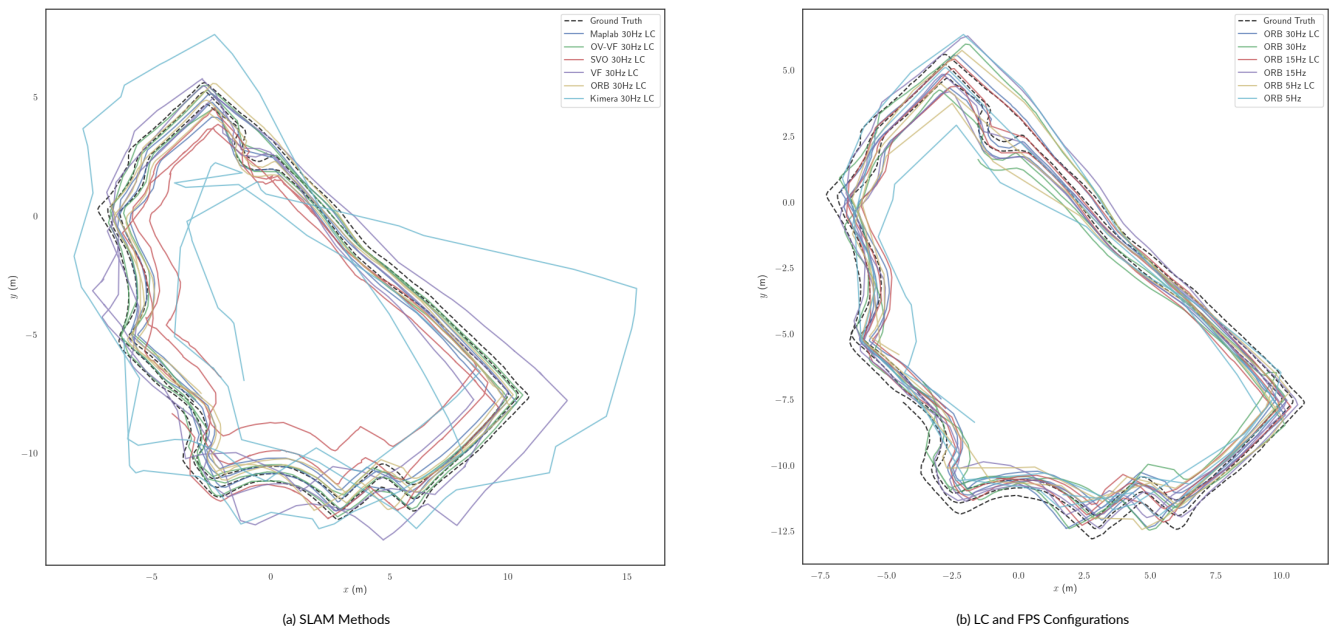


**FIGURE 3** Trajectories for the *Garden Medium Perimeter* scenario: (a) illustrates the comparison of the SLAM methods while (b) shows the differences in LC and FPS configurations of ORB-SLAM3.

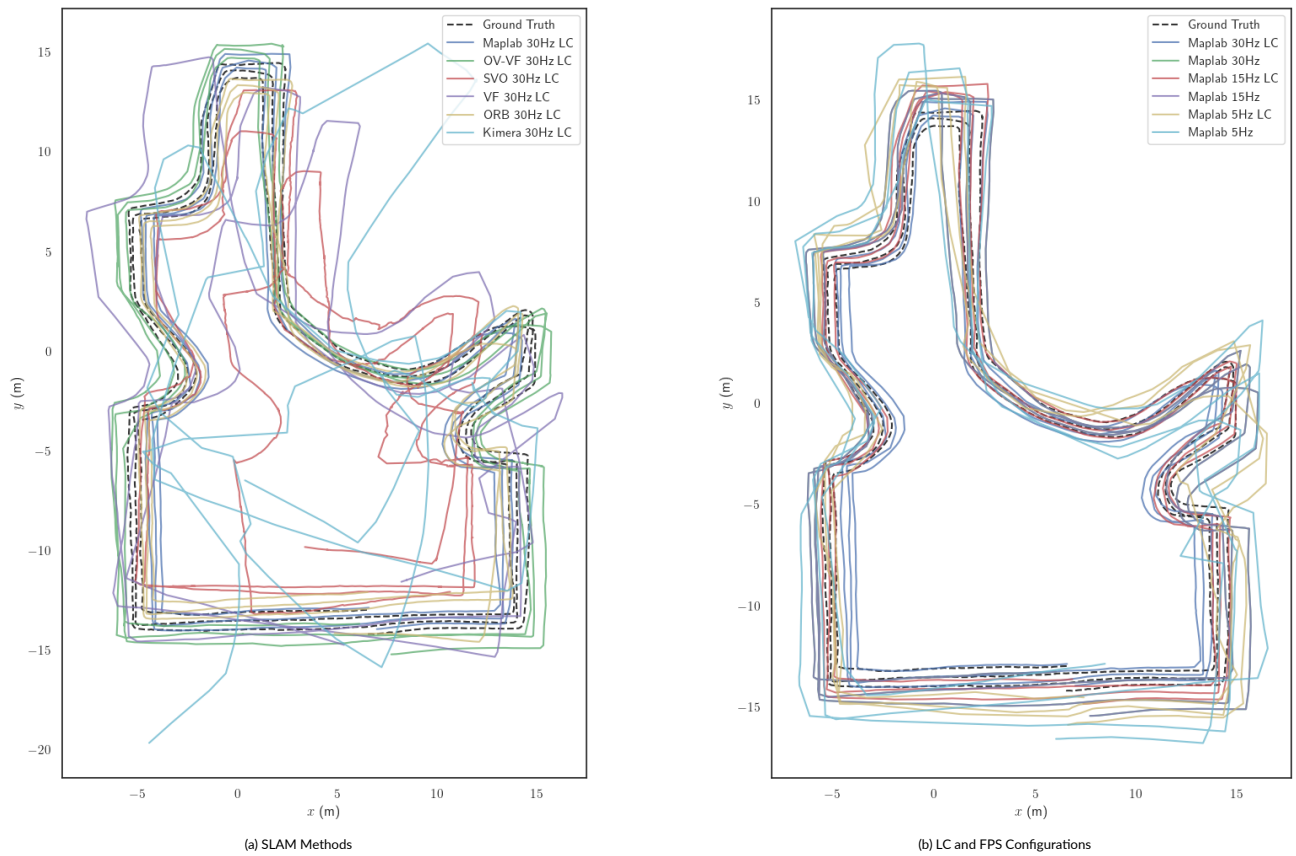


**FIGURE 4** Trajectories for the *Garden Large Perimeter* scenario: (a) illustrates the comparison of the SLAM methods while (b) shows the differences in LC and FPS configurations of OpenVINS + Maplab.

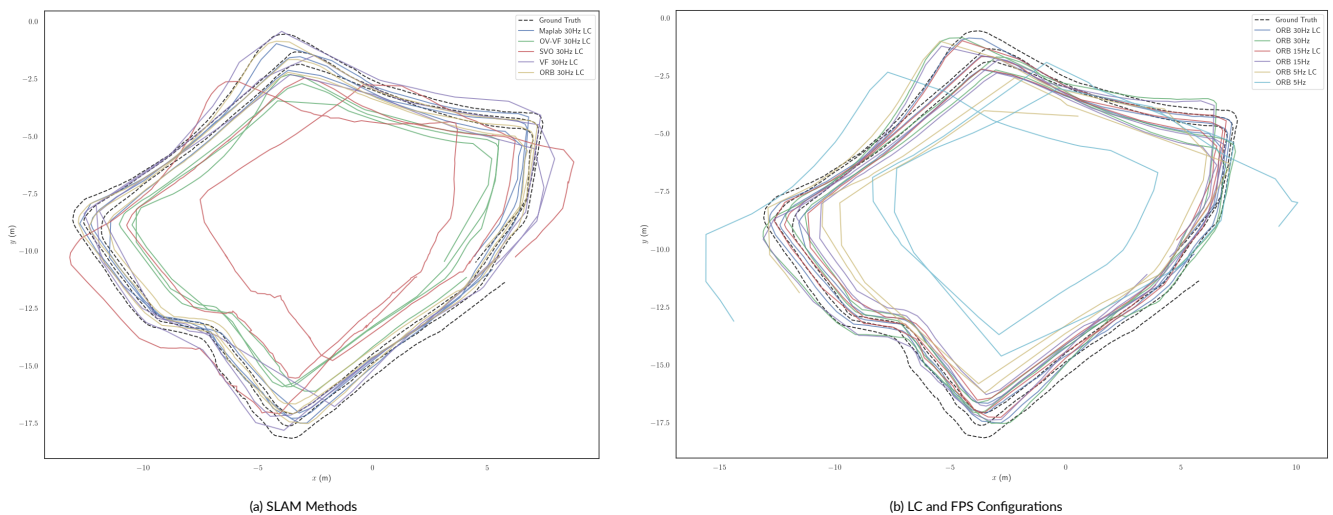


**FIGURE 5** Trajectories for the *Park Perimeter* scenario: (a) illustrates the comparison of the SLAM methods while (b) shows the differences in LC and FPS configurations of ORB-SLAM3.

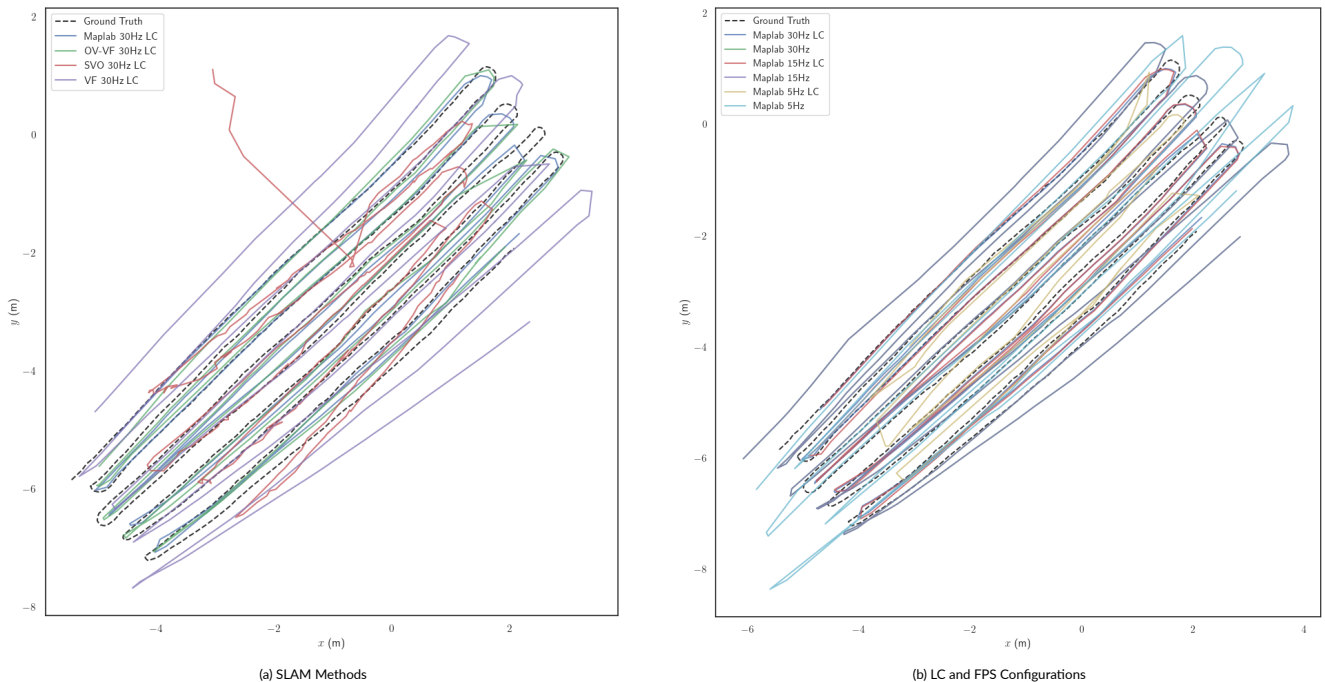


**FIGURE 6** Trajectories for the *Garden Medium Lane* scenario: (a) illustrates the comparison of the SLAM methods while (b) shows the differences in LC and FPS configurations of OpenVINS + Maplab.

In the *Garden Large Perimeter* scenario, OpenVINS + Maplab and OpenVINS + VINS-Fusion maintained accurate trajectories with minor scale issues, depicted in Figure 4a. ORB-SLAM3 experienced scale issues and minor drift, while VINS-Fusion and SVO Pro encountered significant drift. Kimera failed completely in this environment. Comparatively, OpenVINS + Maplab at 30 FPS and 15 FPS with LC, results were consistent with minor scaling issues, but without LC, drift became more apparent. At 5 FPS, trajectories showed significant scaling and drift problems, which worsened without LC, see Figure 4b.

In the *Park Perimeter* scenario, ORB-SLAM3, OpenVINS + Maplab, and VINS-Fusion performed well with minor scale issues. OpenVINS + VINS-Fusion had some scale issues, while SVO Pro experienced significant drift and Kimera failed completely, as visualized in Figure 5a. When comparing different frame rates and LC configurations, see Figure 5b, ORB-SLAM3 showed comparable results at 30 FPS and 15 FPS, both with and without LC, showing minor scale issues. At 5 FPS, the system exhibited pronounced scale inconsistencies and considerable drift when operating without LC.

In the *Garden Medium Lane* scenario, OpenVINS + Maplab and OpenVINS + VINS-Fusion were accurate with minor scale issues and managed 180° rotations effectively, as shown in Figure 6a. VINS-Fusion showed drift during 180° rotations and had scale issues, while SVO Pro had larger scale issues and drifted away towards the end. ORB-SLAM3 and Kimera failed completely. For OpenVINS + Maplab, at 30 FPS and 15 FPS without LC, the results were nearly identical, struggling with scale and drift. With LC, the results improved, showing minor scale issues. At 5 FPS, both with and without LC, we observed significant scale problems, see Figure 6b.

## 4.2 | Computational Efficiency

The implementation of LC significantly impacts the computational resources required by SLAM algorithms. We provide detailed quantitative evaluations for ORB-SLAM3, VINS-Fusion, OpenVINS + VINS-Fusion, Kimera, and SVO Pro of a specific run in the *Garden Medium Perimeter* scenario in Table 5. Note that we did not include values for OpenVINS + Maplab, as Maplab operates offline in a post-processing manner.

ORB-SLAM3 showed the highest CPU usage among all evaluated SLAM methods without LC and a high CPU usage when LC is enabled, indicating that this method is particularly resource-intensive. Without LC, there was a slight decrease in demand, and CPU usage declined as frame rates were reduced. VINS-Fusion exhibited a more moderate CPU usage profile. At 30 FPS, the CPU demand was substantial and LC slightly lowered CPU usage. This usage dropped significantly for lower frame rates. OpenVINS + VINS-Fusion showed varying CPU usage. With LC enabled at 30 FPS, the CPU usage was moderate and consistent. However, without LC, the CPU demand was significantly lower across all frame rates, indicating that the presence of LC greatly impacts the resource requirements. Kimera displayed the highest variability in CPU usage. At 30 FPS with LC, the CPU usage was the highest among all the methods tested. This demand decreased significantly at lower frame rates (15 FPS and 5 FPS). The substantial drop in CPU usage without LC suggests that Kimera's LC module is highly resource-intensive. SVO Pro maintained a moderate CPU usage. At 30 FPS with LC, the CPU demand was manageable and decreased steadily at lower frame rates. Without LC, the CPU usage was consistently lower across all frame rates.

**TABLE 5** CPU and Memory Usage in *Garden Medium Perimeter* scenario with and without LC at 30 FPS, 15 FPS, and 5 FPS. All reported results involve the publicly available open-source implementations.

| Method                    | FPS | LC  | CPU Usage [%] |               |               |               | Memory Usage [GB] |             |             |             |
|---------------------------|-----|-----|---------------|---------------|---------------|---------------|-------------------|-------------|-------------|-------------|
|                           |     |     | Min           | Mean          | Median        | Max           | Min               | Mean        | Median      | Max         |
| ORB-SLAM3                 | 30  | On  | 371.10        | 403.02        | 401.20        | 475.50        | 0.52              | 0.96        | 0.96        | 1.39        |
|                           |     | Off | 369.30        | 400.73        | 399.40        | 451.30        | 0.52              | 0.93        | 0.93        | 1.34        |
|                           | 15  | On  | 281.50        | 315.23        | 315.40        | 350.90        | 0.52              | 0.97        | 0.98        | 1.36        |
|                           |     | Off | 282.00        | 309.97        | 309.00        | 358.90        | 0.51              | 0.94        | 0.94        | 1.32        |
|                           | 5   | On  | <b>227.10</b> | <b>246.91</b> | 247.80        | <b>268.70</b> | 0.52              | <b>0.79</b> | <b>0.79</b> | <b>1.06</b> |
|                           |     | Off | 227.30        | 247.47        | <b>247.10</b> | 273.10        | <b>0.51</b>       | 0.82        | 0.82        | 1.13        |
| VINS-Fusion               | 30  | On  | <b>32.80</b>  | 266.84        | 270.90        | 321.40        | <b>0.09</b>       | 0.11        | 0.12        | <b>0.12</b> |
|                           |     | Off | 58.60         | 243.23        | 236.90        | 365.80        | <b>0.09</b>       | 0.11        | <b>0.10</b> | 0.14        |
|                           | 15  | On  | 109.40        | 138.73        | 139.40        | 173.10        | <b>0.09</b>       | <b>0.10</b> | <b>0.10</b> | 0.11        |
|                           |     | Off | 108.40        | 129.86        | 129.00        | 161.00        | <b>0.09</b>       | <b>0.10</b> | <b>0.10</b> | 0.11        |
|                           | 5   | On  | 37.80         | 48.97         | 48.80         | 59.70         | <b>0.09</b>       | <b>0.10</b> | <b>0.10</b> | 0.11        |
|                           |     | Off | 35.90         | <b>46.72</b>  | <b>46.80</b>  | <b>56.80</b>  | <b>0.09</b>       | <b>0.10</b> | <b>0.10</b> | <b>0.10</b> |
| OpenVINS<br>+ VINS-Fusion | 30  | On  | 7.90          | 139.51        | 135.30        | 235.20        | 0.50              | 3.21        | 3.23        | 5.89        |
|                           |     | Off | <b>2.00</b>   | 65.00         | 65.80         | 95.70         | <b>0.08</b>       | <b>0.29</b> | <b>0.29</b> | <b>0.29</b> |
|                           | 15  | On  | 23.70         | 141.14        | 137.40        | 242.30        | 0.61              | 3.21        | 3.22        | 5.89        |
|                           |     | Off | 10.00         | 55.52         | 55.80         | 87.70         | 0.22              | <b>0.29</b> | <b>0.29</b> | 0.30        |
|                           | 5   | On  | 13.80         | 74.94         | 74.75         | 107.90        | 0.58              | 1.57        | 1.59        | 2.51        |
|                           |     | Off | <b>5.90</b>   | <b>41.75</b>  | <b>43.70</b>  | <b>48.70</b>  | 0.19              | 0.32        | 0.33        | 0.34        |
| Kimera                    | 30  | On  | 66.70         | 638.89        | 625.65        | 1490.00       | 0.56              | 1.37        | 1.38        | 2.07        |
|                           |     | Off | 69.30         | 163.16        | 167.20        | 190.20        | 0.29              | 0.56        | 0.57        | 0.62        |
|                           | 15  | On  | 37.90         | 443.41        | 354.30        | 1111.30       | 0.68              | 1.28        | 1.29        | 1.82        |
|                           |     | Off | 39.70         | 125.49        | 128.70        | 173.80        | 0.21              | 0.35        | 0.35        | 0.39        |
|                           | 5   | On  | 15.00         | 356.38        | 122.00        | 1410.30       | 0.56              | 1.15        | 1.15        | 1.59        |
|                           |     | Off | <b>14.00</b>  | <b>71.89</b>  | <b>70.90</b>  | <b>122.50</b> | <b>0.17</b>       | <b>0.30</b> | <b>0.30</b> | <b>0.34</b> |
| SVO Pro                   | 30  | On  | 60.70         | 289.07        | 295.90        | 351.50        | <b>0.10</b>       | 0.72        | 0.75        | 1.29        |
|                           |     | Off | <b>6.00</b>   | 163.11        | 166.40        | 203.10        | <b>0.10</b>       | 0.18        | 0.18        | 0.18        |
|                           | 15  | On  | 23.90         | 162.30        | 162.50        | 226.20        | <b>0.10</b>       | 0.51        | 0.50        | 0.85        |
|                           |     | Off | 28.90         | 98.51         | 100.80        | 125.60        | <b>0.10</b>       | 0.18        | 0.18        | 0.18        |
|                           | 5   | On  | 10.00         | 52.44         | 52.80         | 71.70         | <b>0.10</b>       | 0.29        | 0.29        | 0.39        |
|                           |     | Off | 11.00         | <b>26.13</b>  | <b>26.90</b>  | <b>31.90</b>  | <b>0.10</b>       | <b>0.17</b> | <b>0.17</b> | <b>0.17</b> |

Regarding memory usage, ORB-SLAM3 used a moderate amount of memory across all frame rates, with minimal differences between configurations with and without LC. Memory usage for 30 FPS and 15 FPS remained at the same level but decreased slightly at lower frame rates, indicating stable memory demands regardless of LC. VINS-Fusion had very low memory usage, consistently maintaining low values across all frame rates and LC configurations. In contrast, OpenVINS + VINS-Fusion displayed significant memory usage at all frame rates, particularly with LC enabled. Without LC, memory usage dropped drastically, highlighting the substantial impact of LC on memory requirements. Kimera showed moderate memory usage, with memory usage higher with LC than without LC across all frame rate, suggesting that Kimera’s memory usage is heavily influenced by the LC process. SVO Pro maintained low to moderate memory usage. The memory demand was higher with LC at 30 FPS but remained reasonable. At lower frame rates, the memory usage decreased, with significant differences between configurations with and without LC.

Overall, ORB-SLAM3 and Kimera are the most CPU-intensive SLAM methods, especially with LC enabled, which significantly increases their resource demands. VINS-Fusion and SVO Pro are more efficient in CPU and memory usage, particularly at lower frame rates. OpenVINS + VINS-Fusion stands out with its high memory usage when LC is enabled, indicating a trade-off between computational efficiency and memory overhead.

## 5 | DISCUSSION

On the impact of LC on SLAM algorithms, our study reveals that, while LC broadly enhances localization accuracy, its influence on computational demands diverges across different systems, see Figure 7. This divergence highlights an essential strategic balance that must be struck between accuracy enhancement and the management of computational resources. Further, the distinction in performance between

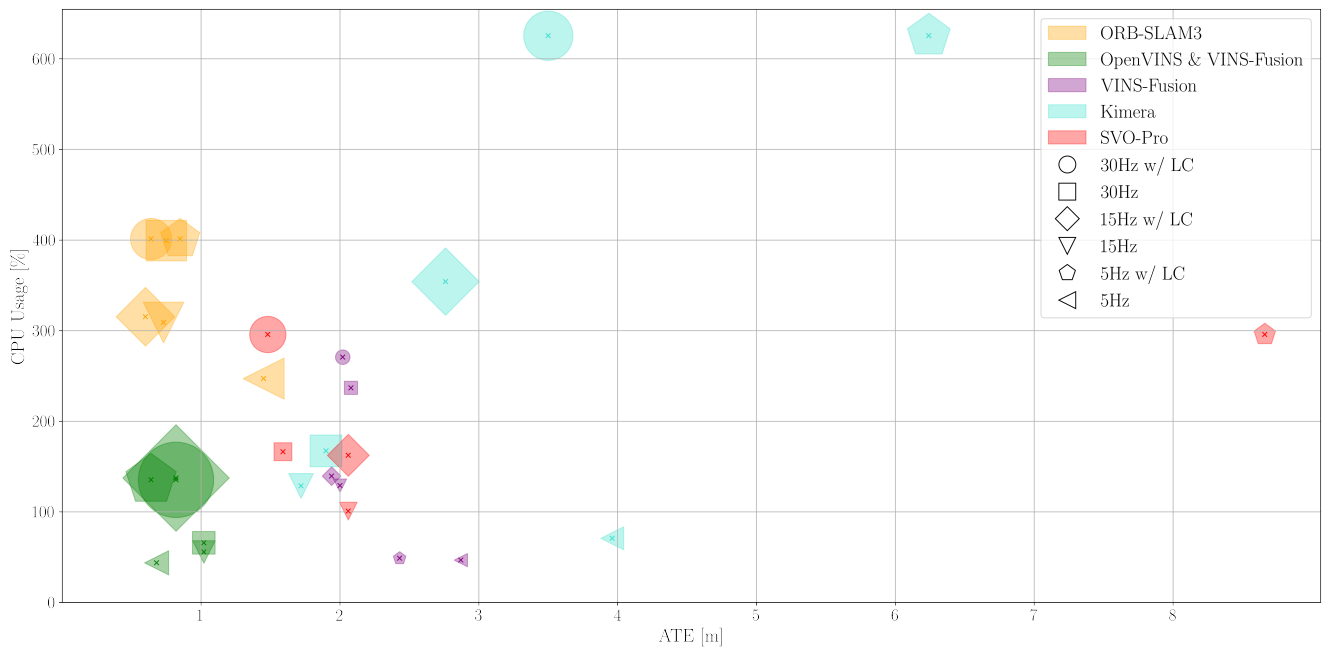


**FIGURE 7** Comparison of CPU utilization versus RMSE ATE for the SLAM methods and their configurations, considering LC and FPS, in the *Garden Medium Perimeter* scenario. Symbol size corresponds proportionally to memory consumption.

driving scenarios, i.e., *Perimeter* and *Lane*, refines our understanding of LC's effects, underlining the importance of context in evaluating SLAM system performance.

**ORB-SLAM3** with LC consistently improved localization accuracy across different scenarios, maintaining low ATE values for both *Perimeter* and *Lane* scenarios. Higher frame rates (30 FPS and 15 FPS) significantly enhanced performance, particularly with LC, while at 5 FPS, the *Lane* scenario performance declined notably. The computational demand was highest with LC enabled at 30 FPS, indicating that ORB-SLAM3 is resource-intensive but offers superior accuracy, making it suitable for scenarios where computational resources are available. Memory usage was quite stable at a moderate level across different LC and FPS configurations, highlighting ORB-SLAM3's stable memory demands. Lower frame rates reduced CPU usage but also compromised accuracy, emphasizing a trade-off between performance and resource consumption. Overall, ORB-SLAM3 demonstrates improvements in accuracy with higher frame rates and LC, though these enhancements come at the expense of increased computational resource utilization.

**VINS-Fusion** demonstrated consistent improvements in localization accuracy with LC, particularly at 30 FPS and 15 FPS. However, the overall localization accuracy was at a medium to low level, struggling especially in the *Lane* scenario and low frame rates. VINS-Fusion exhibited moderate CPU usage, which declined at lower frame rates, and very low memory demands, making it efficient for environments with limited resources. Despite its resource efficiency, VINS-Fusion struggles at lower frame rates and in complex scenarios, suggesting that while it is a

resource-efficient option its accuracy may not be adequate for dynamic or highly complex environments.

**OpenVINS + VINS-Fusion** showed stable performance with LC, particularly at higher frame rates, maintaining a low ATE in the *Perimeter* scenario at 30 FPS and 15 FPS. However, the *Lane* scenario consistently failed. Lower frame rates did not lead to a substantial increase in ATE, which remained moderate. Overall, CPU usage was medium to low, with significant variation when LC was enabled. Memory usage was notably high with LC, indicating a trade-off between computational efficiency and memory overhead. Using LC significantly increased computational demand, resulting in CPU usage that was roughly double and memory usage that was about ten times greater than when LC was not used. This makes LC useful only in applications with no limitations of computational resources, suggesting that OpenVINS + VINS-Fusion with LC is best suited for environments with sufficient computational capacity. The substantial increase in computational demand when integrating OpenVINS with the LC module from VINS-Fusion likely stems from the loosely coupled architecture, which can introduce inefficiencies due to the need for repeated data handling and processing between the two systems. This contrasts with the standalone VINS-Fusion, where the integration of LC is more tightly coupled and optimized for lower overhead. The implementation in OpenVINS + VINS-Fusion may benefit from further optimization to reduce redundancy and streamline data exchange processes, enhancing efficiency without compromising the performance gains provided by LC.

**OpenVINS + Maplab** consistently performed well with LC, especially at higher frame rates, maintaining low ATE values in the *Perimeter*

scenario and showing improved accuracy overall. Lower frame rates increased ATE, particularly in complex scenarios, emphasizing the importance of high frame rates for accuracy. The *Lane* scenario showed improvement with LC but experienced greater difficulties in large environments and at lower frame rates. Operating offline, Maplab avoids real-time computational constraints, ideal for applications with post-processing capabilities. This method is suitable for environments where high computational demand can be managed in non-real-time settings.

**Kimera** exhibits high variance in localization accuracy, demonstrated by elevated ATE values across various environments and particularly in the *Lane* scenario at low frame rates. CPU usage was notably high, especially with LC enabled at 30 FPS, while memory usage ranged from moderate to high. This suggests that Kimera’s high resource utilization does not translate into equivalent accuracy gains, making it less suitable for applications with constrained computational resources.

**SVO Pro** showed improved performance with LC, particularly at higher frame rates, demonstrating reasonable localization accuracy in the *Perimeter* scenario but struggling more with the *Lane* scenario. CPU usage was at a medium level and significantly increased with

LC, while memory usage remained low. SVO Pro benefits from higher frame rates and LC for optimal accuracy, making it suitable for scenarios where medium computational loads are acceptable and higher frame rates can be maintained. However, due to its moderate accuracy and increased computational demands with LC, it may not be ideal for resource-constrained environments.

For agricultural applications, high localization accuracy and efficient computational resource management are crucial. Figure 8 visualizes the main findings of our study regarding the effects of LC and varying FPS on the ATE, CPU, and memory usage. ORB-SLAM3 with LC stands out as the best option. It provides superior precision at higher frame rates, making it ideal for environments that can support the necessary computational demands. OpenVINS + VINS-Fusion is an effective choice for agricultural settings with ample computational capacity. With LC, it maintains low ATE and demonstrates stable performance, making it suitable for detailed field analysis and large-scale agricultural data collection where high memory usage can be accommodated. Additionally, without LC, OpenVINS + VINS-Fusion achieves good accuracy results with a very low computational footprint, making it a suitable choice

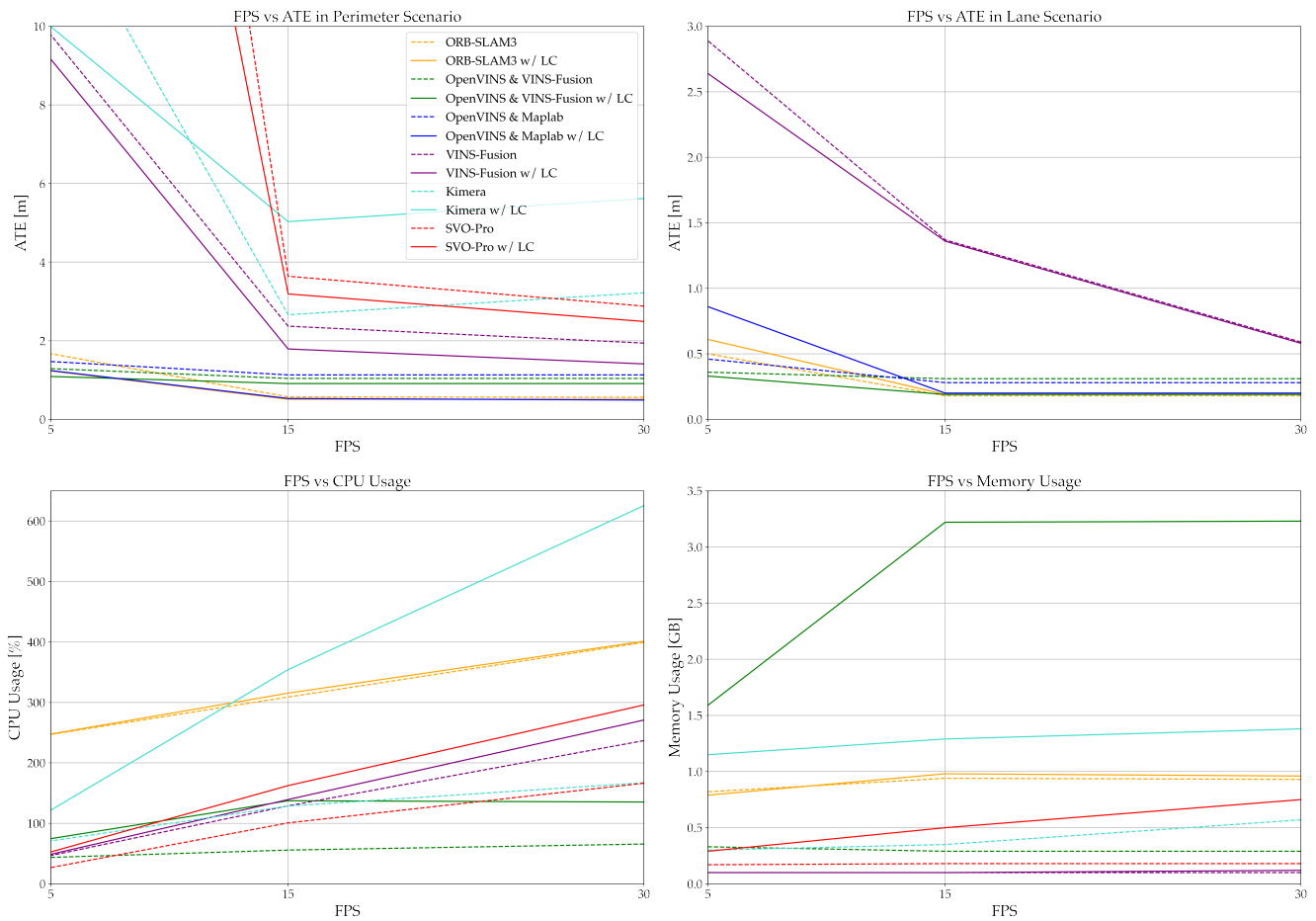


**FIGURE 8** Comparison of SLAM methods regarding ATE in Perimeter and Lane driving scenarios, as well as CPU and memory usage under different FPS, with and without LC.

for embedded solutions with limited computational resources. OpenVINS + Maplab is particularly suited for applications that can handle post-processing. Its ability to offer superior localization accuracy without real-time computational constraints makes it perfect for scenarios where detailed offline analysis of agricultural data is needed, such as post-harvest assessments and long-term crop monitoring.

The comparison between the *Perimeter* and *Lane* scenarios reveals distinct differences in performance across various SLAM algorithms. Notably, the *Lane* scenario exhibits significant variability, displaying high accuracy and superior localization precision in certain environments and methods, such as ORB-SLAM3, OpenVINS + VINS-Fusion, and OpenVINS + Maplab. This suggests a potential for exceptional performance under favorable conditions. However, the same methods also encounter severe challenges in specific environments such as the *Garden Small*, *Medium*, and *Large*, where localization occasionally fails completely, indicating the methods' inability to handle the scenario reliably and lack of robustness. Overall, while the *Lane* scenario shows potential for high precision, its performance is notably inconsistent, making it less robust compared to the *Perimeter* scenario. This inconsistency can be attributed to the demanding nature of the *Lane* scenario, which includes multiple 180° turns. These maneuvers are likely problematic for localization, often leading to drift and contributing to the varied results observed across different SLAM implementations.

## 6 | CONCLUSION

In our investigation of the impact of LC on Visual-Inertial SLAM systems in agricultural and unstructured environments, we thoroughly evaluated ORB-SLAM3, VINS-Fusion, OpenVINS enhanced with VINS-Fusion's and Maplab's LC methods, Kimera, and SVO Pro, while also examining two different driving scenarios, namely *Perimeter* and *Lane*. The results highlight the crucial role of LC in enhancing localization accuracy, especially in unpredictable environments prone to significant drift.

ORB-SLAM3 maintains high localization accuracy, with LC slightly improving it without introducing substantial computational overhead. However, the method requires considerable computational resources at all frame rates, making it suitable for high-precision tasks in resource-rich environments. VINS-Fusion offers moderate localization improvements with LC and struggles at lower frame rates, but its efficient CPU and memory usage makes it viable for resource-constrained applications where high localization accuracy is not required. OpenVINS + VINS-Fusion performs well, with LC slightly improving accuracy but introducing significant computational overhead. Without LC, it remains an efficient choice for embedded systems with limited resources. OpenVINS + Maplab excels in post-processing scenarios, providing high localization accuracy without real-time computational constraints, ideal for detailed agricultural data analysis and long-term monitoring tasks. Kimera faces challenges with localization accuracy and high CPU usage with LC, making it less suitable for resource-constrained applications. SVO Pro

benefits from LC and higher frame rates, maintaining reasonable localization accuracy but struggling with increased computational demands at lower frame rates. Although the *Lane* scenario at times exhibits superior localization accuracy across different environments and SLAM methods, it does not match the robustness of the *Perimeter* scenario, as it frequently encounters failures under more demanding conditions.

Our future research directions will explore deep learning-based LC techniques, specifically incorporating foundation models to robustly detect loops. Additionally, we will focus on enhancing the robustness of SLAM systems under various environmental conditions, including different weather conditions and seasonal changes in agricultural environments. Expanding these findings to broader applications and integrating multi-modal sensor data with SLAM systems could further improve localization accuracy and robustness across diverse scenarios.


## ACKNOWLEDGMENTS

We thank Joshua Uhl for his support during the data capturing and implementation phase, and Frank Holzmüller and Manuel Kaiser for their initial support of the project. We also acknowledge Sabrina Kaniewski for her valuable assistance with reviewing and editing.

## ORCID

Fabian Schmidt 

Constantin Blessing 

Markus Enzweiler 

Abhinav Valada 

## REFERENCES

- Aguiar, A. S., Dos Santos, F. N., Cunha, J. B., Sobreira, H., & Sousa, A. J. (2020). Localization and mapping for robots in agriculture and forestry: A survey. *Robotics*, 9(4), 97. <https://doi.org/10.3390/robotics9040097>.
- Angeli, A., Filliat, D., Doncieux, S., & Meyer, J.-A. (2008). Fast and incremental method for loop-closure detection using bags of visual words. *IEEE Transactions on Robotics*, 24(5), 1027-1037. <https://doi.org/10.1109/TR0.2008.2004514>.
- Arce, J., Vödisch, N., Cattaneo, D., Burgard, W., & Valada, A. (2023). Padloc: Lidar-based deep loop closure detection and registration using panoptic attention. *IEEE Robotics and Automation Letters*, 8(3), 1319-1326. <https://doi.org/10.1109/LRA.2023.3239312>.
- Bahnam, S., Pfeiffer, S., & de Croon, G. C. (2021). Stereo visual inertial odometry for robots with limited computational resources. In *2021 IEEE/RSJ International Conference on Intelligent Robots and Systems (IROS)* (pp. 9154-9159). <https://doi.org/10.1109/IR051168.2021.9636807>.
- Bešić, B., & Valada, A. (2022). Dynamic object removal and spatio-temporal rgb-d inpainting via geometry-aware adversarial learning. *IEEE Transactions on Intelligent Vehicles*, 7(2), 170-185. <https://doi.org/10.1109/TIV.2022.3140654>.
- Bujanca, M., Shi, X., Spear, M., Zhao, P., Lennox, B., & Luján, M. (2021). Robust slam systems: Are we there yet? In *2021 IEEE/RSJ International*

- conference on intelligent robots and systems (iros) (pp. 5320–5327). <https://doi.org/10.1109/IRoS51168.2021.9636814>.
- Burri, M., Nikolic, J., Gohl, P., Schneider, T., Rehder, J., Omari, S., ... Siegwart, R. (2016). The euroc micro aerial vehicle datasets. *The International Journal of Robotics Research*, 35(10), 1157–1163. <https://doi.org/10.1177/0278364915620033>.
- Buyval, A., Afanasyev, I., & Magid, E. (2017). Comparative analysis of ros-based monocular slam methods for indoor navigation. In *Ninth international conference on machine vision (icmv 2016)* (Vol. 10341, pp. 305–310). <https://doi.org/10.1117/12.2268809>.
- Cadena, C., Carlone, L., Carrillo, H., Latif, Y., Scaramuzza, D., Neira, J., ... Leonard, J. J. (2016). Past, present, and future of simultaneous localization and mapping: Toward the robust-perception age. *IEEE Transactions on Robotics*, 32(6), 1309–1332. <https://doi.org/10.1109/TR0.2016.2624754>.
- Campos, C., Elvira, R., Rodríguez, J. J. G., Montiel, J. M., & Tardós, J. D. (2021). Orb-slam3: An accurate open-source library for visual, visual-inertial, and multimap slam. *IEEE Transactions on Robotics*, 37(6), 1874–1890. <https://doi.org/10.1109/TR0.2021.3075644>.
- Cao, S., Lu, X., & Shen, S. (2022). Gvins: Tightly coupled gnss-visual-inertial fusion for smooth and consistent state estimation. *IEEE Transactions on Robotics*, 38(4), 2004–2021. <https://doi.org/10.1109/TR0.2021.3133730>.
- Capua, F. R., Sansoni, S., & Moreyra, M. L. (2018). Comparative analysis of visual-slam algorithms applied to fruit environments. In *2018 argentine conference on automatic control (aadeca)* (pp. 1–6). <https://doi.org/10.23919/AADECA.2018.8577360>.
- Cattaneo, D., & Valada, A. (2024). Cmrnext: Camera to lidar matching in the wild for localization and extrinsic calibration. *arXiv preprint arXiv:2402.00129*. <https://doi.org/10.48550/arXiv.2402.00129>.
- Chahine, G., & Pradalier, C. (2018). Survey of monocular slam algorithms in natural environments. In *2018 15th conference on computer and robot vision (crv)* (p. 345–352). <https://doi.org/10.1109/CRV.2018.00055>.
- Comelli, R., Pire, T., & Kofman, E. (2019). Evaluation of visual slam algorithms on agricultural dataset. *Reunión de trabajo en Procesamiento de la Información y Control*, 1–6.
- Cramariuc, A., Bernreiter, L., Tschopp, F., Fehr, M., Reijgwart, V., Nieto, J., ... Cadena, C. (2022). maplab 2.0—a modular and multi-modal mapping framework. *IEEE Robotics and Automation Letters*, 8(2), 520–527. <https://doi.org/10.1109/LRA.2022.3227865>.
- Cremona, J., Comelli, R., & Pire, T. (2022). Experimental evaluation of visual-inertial odometry systems for arable farming. *Journal of Field Robotics*, 39(7), 1121–1135. <https://doi.org/10.1002/rob.22099>.
- Delmerico, J., & Scaramuzza, D. (2018). A benchmark comparison of monocular visual-inertial odometry algorithms for flying robots. In *2018 IEEE International Conference on Robotics and Automation (ICRA)* (p. 2502–2509). <https://doi.org/10.1109/ICRA.2018.8460664>.
- Filipenko, M., & Afanasyev, I. (2018). Comparison of various slam systems for mobile robot in an indoor environment. In *2018 international conference on intelligent systems (is)* (pp. 400–407). <https://doi.org/10.1109/IS.2018.8710464>.
- Forster, C., Zhang, Z., Gassner, M., Werlberger, M., & Scaramuzza, D. (2017). Svo: Semidirect visual odometry for monocular and multicamera systems. *IEEE Transactions on Robotics*, 33(2), 249–265. <https://doi.org/10.1109/TR0.2016.2623335>.
- Gálvez-López, D., & Tardós, J. D. (2012, October). Bags of binary words for fast place recognition in image sequences. *IEEE Transactions on Robotics*, 28(5), 1188–1197. <https://doi.org/10.1109/TR0.2012.2197158>.
- Gao, B., Lang, H., & Ren, J. (2020). Stereo visual slam for autonomous vehicles: A review. In *2020 IEEE International Conference on Systems, Man, and Cybernetics (SMC)* (pp. 1316–1322). <https://doi.org/10.1109/SMC42975.2020.9283161>.
- Geiger, A., Lenz, P., & Urtasun, R. (2012). Are we ready for autonomous driving? the kitti vision benchmark suite. In *2012 IEEE Conference on Computer Vision and Pattern Recognition* (pp. 3354–3361). <https://doi.org/10.1109/CVPR.2012.6248074>.
- Geneva, P., Eckenhoff, K., Lee, W., Yang, Y., & Huang, G. (2020). Openvins: A research platform for visual-inertial estimation. In *2020 IEEE International Conference on Robotics and Automation (ICRA)* (pp. 4666–4672). <https://doi.org/10.1109/ICRA40945.2020.9196524>.
- Giubilato, R., Chiodini, S., Pertile, M., & Debei, S. (2018). An experimental comparison of ros-compatible stereo visual slam methods for planetary rovers. In *2018 5th IEEE International Workshop on Metrology for Aerospace (MetroAerospace)* (pp. 386–391). <https://doi.org/10.1109/MetroAeroSpace.2018.8453534>.
- Giubilato, R., Chiodini, S., Pertile, M., & Debei, S. (2019). An evaluation of ros-compatible stereo visual slam methods on a nvidia jetson tx2. *Measurement*, 140, 161–170. <https://doi.org/10.1016/j.measurement.2019.03.038>.
- Gosala, N., Petek, K., Drews-Jr, P. L., Burgard, W., & Valada, A. (2023). Skyeye: Self-supervised bird's-eye-view semantic mapping using monocular frontal view images. In *Proceedings of the IEEE/CVF Conference on Computer Vision and Pattern Recognition* (pp. 14901–14910). <https://doi.org/10.1109/CVPR52729.2023.01431>.
- Griffith, S., Chahine, G., & Pradalier, C. (2017). Symphony lake dataset. *The International Journal of Robotics Research*, 36(11), 1151–1158. <https://doi.org/10.1177/0278364917730606>.
- Grupp, M. (2017). evo: Python package for the evaluation of odometry and slam. <https://github.com/MichaelGrupp/evo>.
- Herrera-Granda, E. P., Torres-Cantero, J. C., Rosales, A., & Peluffo-Ordóñez, D. H. (2023). A comparison of monocular visual slam and visual odometry methods applied to 3d reconstruction. *Applied Sciences*, 13(15), 8837. <https://doi.org/10.3390/app13158837>.
- Hroob, I., Polvara, R., Molina, S., Cielniak, G., & Hanheide, M. (2021). Benchmark of visual and 3d lidar slam systems in simulation environment for vineyards. In *Towards autonomous robotic systems: 22nd annual conference, taros 2021, lincoln, uk, september 8–10, 2021, proceedings 22* (pp. 168–177). <https://doi.org/10.1007/978-3-030>



- 89177-0\_17.
- Ibragimov, I. Z., & Afanasyev, I. M. (2017). Comparison of ros-based visual slam methods in homogeneous indoor environment. In *2017 14th workshop on positioning, navigation and communications (wpnc)* (pp. 1–6). <https://doi.org/10.1109/WPNC.2017.8250081>.
- Islam, R., Habibullah, H., & Hossain, T. (2023). Agri-slam: a real-time stereo visual slam for agricultural environment. *Autonomous Robots*, 47(6), 649–668. <https://doi.org/10.1007/s10514-023-10110-y>.
- Joshi, B., Rahman, S., Kalaitzakis, M., Cain, B., Johnson, J., Xanthidis, M., ... others (2019). Experimental comparison of open source visual-inertial-based state estimation algorithms in the underwater domain. In *2019 IEEE/RSJ International Conference on Intelligent Robots and Systems (IROS)* (pp. 7227–7233). <https://doi.org/10.1109/IR0S40897.2019.8968049>.
- Li, R., Lou, Y., Song, W., Wang, Y., & Tu, Z. (2023). Experimental evaluation of monocular visual inertial slam methods for freight railways. *IEEE Sensors Journal*. <https://doi.org/10.1109/JSEN.2023.3301039>.
- Merzlyakov, A., & Macenski, S. (2021). A comparison of modern general-purpose visual slam approaches. In *2021 IEEE/RSJ International Conference on Intelligent Robots and Systems (IROS)* (p. 9190-9197). <https://doi.org/10.1109/IR0S51168.2021.9636615>.
- Mingachev, E., Lavrenov, R., Tsoy, T., Matsuno, F., Svinin, M., Suthakorn, J., & Magid, E. (2020). Comparison of ros-based monocular visual slam methods: Dso, ldslo, orb-slam2 and dynaslam. In *International Conference on Interactive Collaborative Robotics* (pp. 222–233). [https://doi.org/10.1007/978-3-030-60337-3\\_22](https://doi.org/10.1007/978-3-030-60337-3_22).
- Mourikis, A. I., & Roumeliotis, S. I. (2007). A multi-state constraint kalman filter for vision-aided inertial navigation. In *Proceedings 2007 IEEE International Conference on Robotics and Automation* (pp. 3565–3572). <https://doi.org/10.1109/ROBOT.2007.364024>.
- Nayak, A., Cattaneo, D., & Valada, A. (2023). Ralf: Flow-based global and metric radar localization in lidar maps. *arXiv preprint arXiv:2309.09875*. <https://doi.org/10.48550/arXiv.2309.09875>.
- Passalis, N., Pedrazzi, S., Babuska, R., Burgard, W., Dias, D., Ferro, F., ... others (2022). Opendr: An open toolkit for enabling high performance, low footprint deep learning for robotics. In *2022 IEEE/RSJ International Conference on Intelligent Robots and Systems (IROS)* (pp. 12479–12484). <https://doi.org/10.1109/IR0S47612.2022.9981703>.
- Pire, T., Mujica, M., Civera, J., & Kofman, E. (2019). The rosario dataset: Multisensor data for localization and mapping in agricultural environments. *The International Journal of Robotics Research*, 38(6), 633–641. <https://doi.org/10.1177/0278364919841437>.
- Qin, T., Pan, J., Cao, S., & Shen, S. (2019). A general optimization-based framework for local odometry estimation with multiple sensors. *arXiv preprint arXiv:1901.03638*. <https://doi.org/10.48550/arXiv.1901.03642>.
- Rosinol, A., Violette, A., Abate, M., Hughes, N., Chang, Y., Shi, J., ... Carlone, L. (2021). Kimera: From slam to spatial perception with 3d dynamic scene graphs. *The International Journal of Robotics Research*, 40(12-14), 1510–1546. <https://doi.org/10.1177/0278364921105667>.
- Rublee, E., Rabaud, V., Konolige, K., & Bradski, G. (2011). Orb: An efficient alternative to sift or surf. In *2011 International Conference on Computer Vision* (p. 2564-2571). <https://doi.org/10.1109/ICCV.2011.6126544>.
- Schmidt, F., Holzmüller, F., Kaiser, M., Blessing, C., & Enzweiler, M. (2024). Investigating the impact of loop closing on visual slam localization accuracy in agricultural applications. *Advances in Signal Processing and Artificial Intelligence*, 50(162), 152. <https://doi.org/10.13140/RG.2.2.23368.53763>.
- Servières, M., Renaudin, V., Dupuis, A., & Antigny, N. (2021). Visual and visual-inertial slam: State of the art, classification, and experimental benchmarking. *Journal of Sensors*, 2021, 1–26. <https://doi.org/10.1155/2021/2054828>.
- Sharafutdinov, D., Griguletskii, M., Kopanov, P., Kurenkov, M., Ferrer, G., Burkov, A., ... Tsetserukou, D. (2023). Comparison of modern open-source visual slam approaches. *Journal of Intelligent & Robotic Systems*, 107(3), 43. <https://doi.org/10.1007/s10846-023-01812-7>.
- Sturm, J., Engelhard, N., Endres, F., Burgard, W., & Cremers, D. (2012). A benchmark for the evaluation of rgb-d slam systems. In *2012 IEEE/RSJ International Conference on Intelligent Robots and Systems* (pp. 573–580). <https://doi.org/10.1109/IR0S.2012.6385773>.
- Tschopp, F., Schneider, T., Palmer, A. W., Nourani-Vatani, N., Cadena, C., Siegwart, R., & Nieto, J. (2019). Experimental comparison of visual-aided odometry methods for rail vehicles. *IEEE Robotics and Automation Letters*, 4(2), 1815–1822. <https://doi.org/10.1109/LRA.2019.2897169>.
- Tsintotas, K. A., Bampis, L., & Gasteratos, A. (2022). The revisiting problem in simultaneous localization and mapping: A survey on visual loop closure detection. *IEEE Transactions on Intelligent Transportation Systems*, 23(11), 19929–19953. <https://doi.org/10.1109/TITS.2022.3175656>.
- Umeyama, S. (1991). Least-squares estimation of transformation parameters between two point patterns. *IEEE Transactions on Pattern Analysis & Machine Intelligence*, 13(04), 376–380. <https://doi.org/10.1109/34.88573>.
- Vödisch, N., Cattaneo, D., Burgard, W., & Valada, A. (2022). Continual slam: Beyond lifelong simultaneous localization and mapping through continual learning. In *The international symposium of robotics research* (pp. 19–35). [https://doi.org/10.1007/978-3-031-25555-7\\_3](https://doi.org/10.1007/978-3-031-25555-7_3).
- Vödisch, N., Cattaneo, D., Burgard, W., & Valada, A. (2023). Covio: Online continual learning for visual-inertial odometry. In *Proceedings of the IEEE/CVF Conference on Computer Vision and Pattern Recognition* (pp. 2464–2473). <https://doi.org/10.1109/CVPRW59228.2023.00245>.
- Zhao, Y., Smith, J. S., Karumanchi, S. H., & Vela, P. A. (2020). Closed-loop benchmarking of stereo visual-inertial slam systems: Understanding the impact of drift and latency on tracking accuracy. In *2020 IEEE*

---

*international conference on robotics and automation (icra)* (pp. 1105-1112). <https://doi.org/10.1109/ICRA40945.2020.9197003>.